Body-size reductions in dacryoconarid tentaculitoids during Late Devonian warming

Ashley N. Prow-Fleischer[1], Zunli Lu[1], Kimberly C. Meehan[2], Zonglin Yang[1], Linda C. Ivany[1], Jonathan L. Payne[3]

[1]Department of Earth and Environmental Sciences, Syracuse University, 900 S Crouse Ave, Syracuse, New York, 13210, USA

[2]Department of Geological Sciences, University at Buffalo, 190 Founders Prom, Amherst, New York, 14068, USA

[3] School of Sustainability, Stanford University, 397 Panama Mall, Stanford, California, 94305, USA

ABSTRACT

Body size is an essential factor in an organism's survival, and when paired with paleoenvironmental proxies, size trends can provide insights into a lineage's evolutionary responses to changing environmental conditions. This study explores the diversity and body-volume trends of dacryoconarid tentaculitoids, globally abundant marine zooplankton, in the Devonian of the Appalachian Basin (eastern United States), spanning the late Givetian through the middle Frasnian *punctata* carbon isotope excursion. Using statistical approaches to model trends, we find evidence of a gradual, within-lineage reduction in styliolinid adult body sizes starting at the Givetian-Frasnian boundary. This reduction is followed by a significant decrease in both adult and initial chamber volumes during the *punctata* excursion. At the Givetian-Frasnian boundary, annulated forms (nowakiids) become rare and smooth forms (styliolinids) begin to dominate the assemblage. Using pre-existing geological and geochemical datasets, we consider environmental factors, including sea level, anoxia, nutrient availability, and temperature, as potential drivers of

body-size reductions. Bottom-water anoxia most likely did not influence body-sizes trends of this pelagic group, but frequent water-column overturning in the Frasnian or other exchange between deep and shallow water may have affected taxonomic composition, favoring styliolinids. Sea-surface temperature correlates inversely with body size, suggesting that warming beginning in the early Frasnian may have contributed to gradual, long-term size reductions. Rising temperatures through the middle Frasnian may have led to the disappearance of dacryoconarids in the northern Appalachian Basin after the excursion.

1. INTRODUCTION

Studies of body-size trends over time offer insights into ecological and environmental controls, such as temperature and biogeography, on macroevolutionary patterns within lineages (Hunt, 2007; Payne and Heim, 2020) and, when paired with proxies for environmental conditions, provide constraints on physiological traits in extinct groups (Morten and Twitchett, 2009; Yamaguchi et al., 2012; Rita et al., 2019). Dacryoconarids are a subclass of tentaculitoids, an enigmatic group of conically shaped calcareous zooplankton with biostratigraphic importance for the Devonian System (Fig. 1; Bouček, 1964; Schindler, 2012; Becker et al., 2020). Globally, dacryoconarids reached a maximum in average adult conch volume during the Emsian stage of the Early Devonian (Wei, 2019). After that, the lineage rapidly declined in both average size and taxonomic diversity (Wittmer and Miller, 2011; Wei et al., 2012) before going extinct early in the Famennian (Bond, 2006). Here we report, body-size trends in dacryoconarids from the late Givetian (ca. 382 Ma) to their disappearance in the Northern Appalachian Basin in the middle Frasnian (ca. 374Ma) and conclude that temperature was an important driver of size reduction during the Late Devonian.

2.1 MATERIALS AND METHODS

2.1 Study Area and Samples

The sedimentary successions examined were deposited in an offshore setting of the semi-restricted northern Appalachian Basin which was situated approximately 20°S during the Middle to Late Devonian (Fig. 2a, b; Scotese and McKerrow, 1990; Ver Straeten, 2023). Erosion during the early Frasnian removed approximately 5 m.y. of the record spanning the late Givetian upper *Polygnathus varcus* conodont zone to the early Frasnian *Palmatolepis fasiovalis* zone resulting in the laterally extensive Taghanic Unconformity (Zambito et al., 2016). In the early to middle Frasnian, three second-order transgressive-regressive (TR) cycles - the Genundewa (IIa), Middlesex (IIb), and Rhinestreet (IIc) - controlled basin depth, bottom-water restriction, and connectedness with the open ocean (Fig. 3; Johnson et al., 1985; Becker et al., 2016).

Northern Appalachian Basin localities in Erie County, western New York, preserve a nearly complete sequence of Late Devonian rocks. Comprehensive sedimentological (Johnson et al., 1985; Over et al., 2023), stratigraphic (Klapper and Kirschgasser, 2016), and geochemical (Murphy et al., 2000; Sageman et al., 2003; Lash, 2019) studies of this succession provide important context for exploring the mechanisms behind dacryoconarid body-size changes. Eighteen Mile Creek, approximately 20 km south of Buffalo, NY (Fig. 2) flows east to west and erodes into progressively older strata as it nears the shore of Lake Erie (Grabau, 1898). Five outcrops (A-E) were sampled at low flow, beginning with the upper Windom Shale Member of the Moscow Formation and ending with the lower Angola Shale of the West Falls Group, yielding a composite section spanning the late Givetian to middle Frasnian (Table 1; Brett, 1974; Baird et al., 2006; Over et al., 2023). Thirty hand samples were collected at roughly 0.5 m intervals. Sampling density was increased to every ~0.15 m for 3 samples in the Genundewa Limestone section so as to capture the ~20 centimeter thick styliolinid marker bed (Baird et al., 2006; Over et al. 2023). The bottom 3 m of the Cashaqua Formation were not sampled due to inaccessibility.

Lash (2019) reported organic carbon isotope, total organic carbon and Mo concentrations at Eighteen Mile Creek near sites B and C (Fig. 1a), spanning the West River Formation through the lower Rhinestreet Formation. A positive carbon isotope excursion was identified roughly coinciding with the Middlesex IIb TR cycle transgression and spanning the *Palmatolepis transitans* - *Palmatolepis punctata* conodont biozones. Recognized as the *punctata* carbon isotope excursion, this excursion has been recognized worldwide and is proposed to have been driven by volcanic activity that stimulated productivity and led to enhanced carbon burial (Yans et al., 2007; Morrow et al, 2009; Pisarzowska et al., 2020).

2.2 Laboratory Procedures

Dacryoconarid fossils were extracted following procedures modified from Prow et al. (2023). Approximately 50 grams of material was roughly crushed with a percussion mortar and separated into different granulometric fractions using stacked sieves. The rock fragments ranging from 1.0 to 5.0 cm were processed by saturating in deionized water overnight, decanted, and frozen to -5°C. The frozen fragments were simmered for 20 minutes in a warm solution of 5% Na_2CO_3 in a heat-resistant test tube submerged in a hot water bath. The processed material was wet-sieved to remove residue, dried at 40°C, and searched for fossils. Only intact specimens, having an unfractured aperture and retaining the initial chamber, were chosen for measurement.

Because dacryoconarids are typically found oriented along bedding planes, abundance was estimated using methods from Rita et al. (2019) by counting the number of specimens per unit area (dacryoconarids per square decimeter, specimens dm^{-2}). Dacryoconarids can occur in rock-forming quantities and, therefore, be uncountable, so a numeric value of 1 to 5 was assigned to represent ranges, with 1 being less than 5 specimens per dm^{-2} and 5 representing rock-forming quantity.

A total of 730 dacryoconarids was photographed using a Leica microscope at magnifications of 3x - 5.5x with an attached digital camera and measured in ImageJ software (Version 1.54g; Ferreira and Rasband, 2012). A stage ruler with 0.01 mm precision, the thickness of a dacryoconarid shell (Brocke et al., 2016), was used to calibrate the pixels per mm at each magnification. The long axes of the specimens were oriented normal to the camera lens by leveling in sand. Scanning electron microscopy was performed on a JEOL 6000 series benchtop microscope to observe fine surface structures, such as longitudinal furrows, that distinguish the genera.

2.3 Computational and Statistical Methods

2.3.1 Volume calculations

The dimensions and geometries of conchs were calculated from linear measurements using simple geometric approximations. Initial chamber volume was estimated using the equation for a sphere ($4/3\ \pi r^3$), where *r* is the radius taken from the maximum initial chamber width as measured perpendicular to the longitudinal axis as diameter (2r) (Fig. 1a). While some dacryoconarid initial chambers are ellipsoidal, this spherical approximation was made because the constriction that distinguishes between the chamber and conch is commonly indiscernable (Wei, 2019). The adult length was taken as the length of the entire specimen from the initial chamber tip to the aperture rather than from the beginning of the adult stage. The initial chamber tip was used because not all species have a change in growth angle such that the juvenile stage can be discerned. Adult volume was estimated using the equation of a cone ($h\pi r^2/3$) using the full length (h) and aperture width (2r). Proximal growth angles, used as a characteristic for identification, were taken as the average of three measurements of the first few mm after the initial chamber to account for human error in perceiving the boundary between the adult and juvenile stages (Larsson, 1979).

Because these fossils come from shales, some compaction of the distal (apertural) end may have occurred, whereas the apical end is rarely compacted (Bouček, 1964). This compaction is identified by the appearance of a medial longitudinal groove starting from the aperture. If the specimen is only compacted by no more than half its length, a mathematical correction can be applied which estimates the unaltered proximal growth angle, $\alpha_{corrected}$ (Bouček, 1964) where

$$\alpha_{corrected} = \sin^{-1}\left(\frac{\alpha_{measured}}{length}\right). \quad (1)$$

The corrected aperture diameter can be estimated from the circumference of a circle with

$$\alpha_{corrected} \sim \frac{2\alpha_{measured}}{\pi}. \quad (2)$$

To determine if this approximation was reliable, comparisons were made between three distally flattened specimens of similar length (within ±0.3 mm) to an undeformed specimen with the same morphological features (Table S1 in the Supplemental Material[1]). The correction overestimates the true aperture by no more than 0.05 mm. This determination is further corroborated by the fact that dacryoconarids begin to grow subcylindrical into adulthood, and longer specimens may be more distally flattened regardless of compaction (Bouček, 1964; Wei, 2019).

2.3.2 Taxonomic composition

Body-size trends can be driven by both within-lineage shifts and the disappearance or origination of new taxa over time (e.g., Rego et al., 2012). Here we compare monophyletic groups that have historically been characterized as genera (Bouček, 1964). The contribution of each group was quantified for every consecutive stratigraphic level, *t*, using the approach of Rego et al. (2012) and the following equations by Rita et al. (2019):

$$assemblage\ size\ shift = assemblage\ mean\ size_{bed\ t+1} - assemblage\ \ mean\ size_{bed\ t}, \quad (3)$$

$$within - lineage\ effect = boundary\ crossers\ mean\ size_{bed\ t+1} - boundary\ crossers\ mean\ size_{bed\ t}, \quad (4)$$

$$disappearance\ effect = boundary\ crossers\ mean\ size_{bed\ t} - all\ taxa\ mean\ size_{bed\ t}, \quad (5)$$

$$apperance\ effect = all\ taxa\ mean\ size_{bed\ t+1} - boundary\ crossers\ mean\ size_{bed\ t+1}. \quad (6)$$

Where "boundary crossers" are taxa that appear in stratigraphically successive beds *t* and *t+1,* and "all taxa" are those that appear in the designated interval (e.g. *t+1).*

2.3.3 Statistical method

Differences between measurements made by two data collectors were assessed to ensure no systematic bias. Both individuals measured the volumes of the same dacryoconarids from a subset of 30 randomly sampled images, and Kendall's tau correlation (e.g. Harnik et al. 2017) was used to identify any consistent offset between their respective measurements that might skew results.

To determine whether the assemblage-scale body sizes differed significantly between the *punctata* excursion interval and background conditions, the size distributions at each stratigraphic level were log-transformed and grouped into 'before excursion' and 'during andafter excursion' categories. Because a Shapiro-Wilk test failed to establish normality of the distributions, the hypothesis that the median volumes during the excursion are smaller than those before was tested

using a non-parametric Mann-Whitney U test at a significance level of $\alpha = 0.05$ (Hammer and Harper, 2005). A data point from the Genundewa styliolinid horizon is excluded based on perceived taphonomic alteration (see Appendix : Extended Discussion, Potential Facies Control on Size Distributions section). Statistical analyses were carried out using the OriginLab 2023 software (https://www.originlab.com/).

2.3.3 Evolutionary Trajectory Modeling

To detect whether gradual evolutionary trends toward new trait optima are present in the data we used evolutionary trajectory modeling. The R package paleoTS (version 0.5.3) was used to fit three stochastic evolutionary models to the time-series mean-volume data to assess the significance of any directionality (Hunt, 2022). Under neutral genetic drift, populations evolve according to Brownian or random-walk processes from an ancestral population with an initial trait value of i_0 (Hunt, 2007; Hunt et al., 2015). The null or unbiased random-walk model thus draws a random change in the trait value for the next time step from a Gaussian distribution of the mean (μ) of 0 and variance σ^2_{step} based on the variance of the dataset (Hunt et al., 2015). The biased, or directional, random walk is a process where the next step direction is determined randomly and independently from that of the previous step thus allowing for incrementation of the trait value around a non-zero change in its mean value, μ_{step}. The Ornstein-Uhlenbeck process is a modification of the biased random-walk model where traits are attracted to an optimal value, θ (Hansen, 1997; Hunt et al., 2015). A new parameter, α, is introduced which is a measure of the strength of return toward the optimal value. The directed random-walk process is a linear model, whereas the Ornstein-Uhlenbeck process gives a smooth, continuous curve.

The paleoTS algorithm uses maximum likelihood to estimate the best-supported parameter values that fit the discrete time-series trait data to each model. The Akaike information criterion

(AIC) corrected for sample size (AICc), which considers the number of parameters used in constructing the model, is used to identify the best-fitting model. AICc scores are converted to AIC weight percentages representing the proportional support for each model relative to the maximum likelihood estimation, where a larger percentage indicates a better fit.

Due to uncertainties in relative age dating and the duration of the *punctata* zone (600 k.y.: Kaufmann, 2006; versus 1.3 m.y.:, Becker et al., 2016), we modeled the best-fit adaptive trajectories for adult volume using stratigraphic level. The Genundewa Limestone measurement was excluded from analyses (see section 2.3.3)

2.3.4 Geochemical Data for Basin Anoxia and Nutrient Abundance

Published geochemical proxy data for redox conditions and extent of clastic input (percent totalt organic carbon[TOC], total organic N and P concentrations, Ti/Al, and redox-sensitive trace-metal concentrations), measured from a core near the study area were used to constrain the degree of bottom-water anoxia, ventilation, and connectedness with the open ocean in the northern Appalachian Basin (Murphy et al., 2000; Sageman et al., 2003). Mo concentrations over 25 ppm can indicate anoxic conditions but are alone inconclusive due to hydrogeographic or sedimentological factors that might concentrate Mo (Algeo and Lyons, 2006). The covariation of Mo and TOC is an indicator of basin restriction and dominant controls on organic matter burial where low values of [Mo]/TOC ratio (< 5 ppm per % TOC) indicate restricted settings and intermediate values (between 10-25) are indicative of occasional overturning with intermittent bottom-water anoxia (Algeo and Lyons, 2006). We plot the covariation in adult and initial chamber volumes with Mo/TOC and Mo concentration during each conodont biozone of the early Frasnian to test for a relationship between size and anoxia.

Changes in nutrient availability in the Appalachian Basin were evaluated from total P and N during this study interval (Sageman et al., 2003). Organic matter in mudstones is predominantly derived from marine phytoplankton and has a C:N:P composition approximating the Redfield ratio (106:16:1; Redfield, 1958). Any deviation in sedimentary C:N:P content from the Redfield ratio indicates remobilization from the sediment or enhanced terrestrial delivery (Sageman et al., 2003).

2.3.5 Sea Surface Temperature Reconstruction

Using the Joachimski et al. (2004) conodont apatite composite dataset from epeiric seas within the tropics (0 to 30° paleolatitude), we reconstructed sea-surface temperature during the studied interval using the phosphate-water fractionation regression equation

$$T(°\mathrm{C}) = 118.7\ (\pm 4.9) - 4.22\ (\pm 0.20)(\delta^{18}O_p - \delta^{18}O_w)\ , \qquad (7)$$

where $\delta^{18}O_p$ is the isotope ratio of conodont apatite relative to Vienna standard mean ocean water (V-SMOW), and the $\delta^{18}O_w$ is the estimated Late Devonian global seawater oxygen isotope composition assuming a value of -1‰ due to lack of substantial ice sheets (Pucéat et al., 2010; Becker et al. 2020).

4. RESULTS

4.1 Body-Size Trends

Measurements made by different investigators correlate strongly (Kendall correlation = 0.905), suggesting that human bias does little to skew the results. Excluding for the Genundewa styliolinid horizon, composed almost entirely of a single species of small-chambered styliolinid (Fig. 4g), assemblage-scale mean adult volume trends display a gradual decline from the late Givetian through the early Frasnian with a more rapid shift toward lower average volumes occurring after the onset of the *punctata* excursion at the discontinuity between the Middlesex and

Cashaqua Formations (Figs. 3; and Fig.S1[see footnote 1]). Average adult volumes decrease during the excursion, and they remain lower than pre-excursion values until dacryoconarids disappear in the Appalachian Basin in the upper Rhinestreet Formation. Assemblage-scale initial chamber volumes are variable but tend to correlate with adult volumes. Initial chamber volumes diminish during the *punctata* excursion core but return to larger values during its recovery phase (Fig. 3 and Fig. S2). Both adult volumes (p-value = 0.0009) and initial chamber volumes (p = 0.02) are statistically smaller during the *puncata* interval compared to background times using the Mann-Whitney U test. There is a significant positive relationship between adult and initial chamber volumes (Pearson r = 0.65, p-value <0.001).

4.2 Evolutionary Trajectory Modeling

Among the three models tested, the Ornstein-Uhlenbeck process accounts for 68% of the AICc weight percent for adult volumes, suggesting that dacryoconarid adult volumes trend toward a smaller average size up section (Table 2, Fig. 5). The best-fitting model for initial chamber volume is the directional random walk (73% AIC wt. %; Table A2; Fig. A3), followed by the Ornstein-Uhlenbeck process (18%). This suggests that initial chamber volumes gradually declined through the early Frasnian but not toward a new average trait value that can be identified with the data at hand.

4.3 Occurrences, Diversity, and Abundance

Dacyroconarids were found in most sampled intervals (22 of 30) but were not observed in black shales in the basal 0.5 m of the Middlesex and Rhinestreet Formations or in the lower 4 m of the Angola Shale. The location of the last occurrence of dacryoconarids in the Angola Shale is consistent with the last appearance datum for the styliolinds in the northern Appalachian Basin

(Fig. 3; Yochelson and Kirchgasser, 1986). In the Middlesex and Rhinestreet Formations, approximately 0.5 to 1 m above their bases, dacryoconarids counted on bedding planes exceed 25 specimens dm^{-2}. Except for the Genundewa styliolinid packstone, where dacryoconarids occur in rock-forming quantities, the *punctata* excursion interval contains higher abundances of dacryoconarids distributed throughout the matrix compared to the other units of similar lithology.

Four genera belonging to three families are recognized: *Nowakia* and *Viriatellina* (Nowakiidae), *Striatostyliolina* (Striatostyliolinidae), and *Styliolina* (Styliolinidae; Fig 4). The Givetian had a higher proportion of annulated nowakiid forms compared to the Frasnian, comprising up to 60% of the assemblage (Fig. 6). Family-level turnover occurs in assemblage composition near the Givetian-Frasnian boundary, where annulated forms disappeared. The Genundewa Limestone is likely composed of a single genus *Styliolina* (Fig. 4G) and is delineated by two barren intervals (Fig. 3). There is a stratum-specific occurrence of a nowakiid, possibly *Viriatellina,* in the basal half-meter of the overlying West River Formation (Fig. 4D; Lindemann and Yochelson, 1984). No genus-level turnover was observed during the *punctata* excursion, which was dominated by the smooth varieties *Styliolina* and *Striatostyliolina* (Fig. 4F).

We quantify the family-level within- and among-lineage size shift to dacryoconarid mean adult sizes for each consecutive bed and find that most of the size reduction at the Givetian-Frasnian boundary is due to a within-lineage size shift in surviving taxa mostly belonging to Styliolinidae (Figs. 7, Fig. S4). The large size reduction associated with the disappearance of the Nowakiidae at the Givetian-Frasnian boundary is counterbalanced by the origination of Striatostyliolinidae. During the *punctata* excursion, there are no originations or extinctions, so size reductions are driven by within-lineage shifts in Styliolinidae and Striatostyliolinidae.

4. Basin Anoxia and Nutrient Availability

There are no clear trends between extent of bottom-water anoxia (Mo concentration) and shell volume during either life stage (Fig. 8), but only styliolinids are present when there is evidence for overturning circulation of anoxic water masses (high [Mo]/TOC; Sageman et al., 2003). Assemblage-scale initial chamber volumes are highly variable before the *punctata* excursion, but the mean initial chamber size in Styliolinidae increases gradually through the Frasnian (Fig. S4). An increase in assemblage and within-Styliolinidae initial chamber size during the upper Middlesex Formation coincides with an increase in nutrients (Fig. S4).

4.5 Sea Surface Temperature

Assemblage-scale and the genus *Styliolina* adult volumes show an inverse relationship with sea-surface temperature from the Givetian to the middle Frasnian (Fig. 9).

5. DISCUSSION

Our investigation of dacryoconarid morphology and turnover in the Devonian Appalachian Basin reveals a gradual trend toward smaller sizes in assemblage-scale initial chamber and adult volumes through the early Frasnian. Comparatively rapid reductions in both life stages occur during the *punctata* excursion. Several factors including environmental (e.g. nutrients, basin anoxia; Schöne, 1999; Harnik et al. 2017), climatological (e.g. temperature; Gillooly et al. 2001), ecological (e.g. competition, reproductive strategies; Vance, 1973), and geographical (e.g. range size, sea level; Gaston and Blackburn, 1996) have been shown to influence size distributions in marine invertebrates. Because little is known about the ecological role of dacryoconarids, we are not able to address this potential driver besides considering taxonomic controls on size.

Due to the sampling gap at the bottom of the Cashaqua Formation, we are not able to fully assess the nature of the apparent rapid reduction in size during *punctata* excursion, and instead

focus on the long-term trends. Taphonomic, facies, and taxonomic controls on size shifts are ruled out as primary contributors to overall trends because they only operate at specific stratigraphic horizons, primarily in the early Frasnian West River Formation (Appendix II: Extended Discussion). Conflicting trends between proxy data for nutrient inventory and body-size trends between life stages, in addition to evidence for normal-marine nutrient concentrations during the deposition of the Cashaqua Formation, suggest other climate or environmental factors influenced dacryoconarid sizes at least in the Appalachian Basin (Fig. S4; Appendix: Extended Discussion). We focus on sea level, the extent of bottom-water anoxia, and global sea-surface temperatures as plausible drivers of size reductions.

5.1 Sea Level

Wei (2019) reported an inverse relationship between the Johnson et al. (1985) sea level curve and global tentaculitoid generic diversity, geographic range, and body volumes. They suggested that sea level was a controlling factor in dacryoconarid size reductions, inferred from correlation between diversity and body-volume trends, through the Devonian. However, in the studied section there is no clear relationship between volume and relative sea level (Fig. 3).

The Johnson et al. (1985) sea-level curve is a composite of sedimentary facies data integrated over all of North America and Europe, and therefore likely does not accurately reflect changes in local relative sea level within the tectonically active Appalachian Basin proper. Nevertheless, localities at Eighteen Mile Creek were used in that reconstruction, and the correlation of transgressions with intervals of black shale and limestone in the basin suggests that the broad pattern is at least robust. That a relationship between the Johnson et al. curve and dacryoconarid body size cannot be established suggests that some other environmental factor is at play.

5.2 Basin Anoxia

Because the *punctata* excursion has been linked with higher productivity marked by replacement of oxic facies with black-shale deposition (Pisarzowska et al., 2020), we further examine the potential influence of increased basin anoxia and nutrient abundance on body size. Geochemical data suggest that Appalachian Basin bottom water was only occasionally dysoxic during the core of the *punctata* excursion ([Mo] = 2.1 ppm). In contrast, basin deepening during the Middlesex Formation *transitans* zone and Rhinestreet Formation *Palmatolepis hassi* zones led to greater restriction and persistent anoxia (Sageman et al., 2003). Mo/TOC ratios through the early Frasnian, however, suggest frequent episodes of vertical mixing. The lack of covariation of size with any redox proxy suggests that neither degree of bottom-water anoxia nor basin restriction are likely drivers of the paired reduction in the initial chamber and adult volumes during the excursion or through the Frasnian.

Bottom-water anoxia indicators may not capture the redox conditions experienced by dacryoconarids if they were planktonic but if dacryoconarids did experience suboxic conditions, they might have tolerated them by growing thinner shells (Schindler, 2012; Wei, 2019). During the late Eifelian *otomari* crisis, named for the disappearance of the index species *Nowakia otomari*, oxygen restriction may have led to the extirpation of more ornamented and thicker-shelled forms, while some styliolinids persisted (Schöne, 1999). Wei (2019) found no general temporal or evolutionary trend in shell thickness within any group of tentaculitoids but postulated that thin-walled varieties (dacryoconarids and homoctenids) were adapted to more variable redox conditions, whereas thick-walled *Tentaculites* preferred shallower, oxygen-rich environments (Schöne, 1999). The presence of only smooth varieties in the Appalachian Basin during the early Frasnian with variable bottom-water redox state and frequent overturning may suggest

inhospitable conditions for annulated forms. This interpretation is supported by the stratum-specific occurrence of a nowakiid in the oxygenated West River Formation (Fig. 4).

5. 3 Sea-Surface Temperature

Temperature strongly influences metabolism in ectotherms thus affecting growth rate and maximum size, hypoxia sensitivity, levels of activity, and ultimately, lifespan (Gillooly et al., 2001; Angilletta et al., 2004; Deutsch et al., 2022). While there is no universally accepted mechanism to explain the strong relationship between temperature and body mass, increasing rearing temperatures commonly lead to a predictable decrease in body mass over a biologically relevant temperature range of 0 to 40 °C in aquatic ectotherms (Sibly and Atkinson, 1994; Angilletta et al., 2004).

Bergmann's Rule predicts that larger varieties are typically found at higher latitudes within widely distributed groups (Atkinson et al., 2019), such as tentaculitoids, due to thermally controlled differences in growth rate (Wilson, 2009). While not all organisms, particularly ectotherms, conform to this pattern (Meiri and Dayan, 2003), temperature-controlled size differences cannot be excluded as a possible explanation for the global body size trends reported by Wei (2019) if loss of larger-bodied taxa was associated with latitudinal range contraction in the Late Devonian (Wittmer and Miller, 2011). Alternatively, an intraspecific shift toward smaller body size in a dominant cosmopolitan species, such as *Styliolina fissurella*, in response to warming temperatures may also account for global trajectories.

Pelagic paleotemperature estimates increase over the late Middle to earlyLate Devonian (Fig. 9), Joachimski et al. 2004), with some approaching the thermal limit for most aquatic ectotherms (>40°C; Cereja, 2020). Uncertainty over seawater $\delta^{18}O$ values in epeiric settings (Montañez et al., 2018; Jimenez et al., 2019) means that calculated paleotemperatures could be overestimated.

However, sea-surface temperatures in epeiric seas tend to be more variable and higher compared to the open ocean today (Judd et al., 2020), so such warm values might not be unreasonable for the tropics under the Late Devonian continental configuration and in a greenhouse climate (Joachimski et al. 2009).

The Givetian-Frasnian warming trend commenced with the Taghanic overheating anomaly near the bottom of the study interval (Aboussalam and Becker, 2011). Warming was associated with regional extinctions and migrations and greater cosmopolitanism of pelagic groups like dacryoconarids (Becker et al., 2020) and is coincident with the disappearance of the Nowakiidae in the study area. Warming is also suggested by the presence of large cladoxyl trees in the Catskill Delta, New York, during the Middlesex TRIIb (Rettallack and Huang, 2011). The warming trend may have been interrupted by a brief cooling episode of 3 to 5 °C in the tropics starting in the late *transitans* zone and ending in the early *hassi* zone, due to CO_2 drawdown suggested by $\delta^{18}O_{apatite}$ both from localized ocean-facing sites (Pisarzowska and Racki, 2012) and in composite global datasets (Joachimski and Buggish, 1993). However, the climatic context of the *punctata* excursion is still debated especially in the Northern Appalachian basin where lowering of base level during deposition of the Cashaqua Formation may have dampened the global signature of the event (Lash, 2019). Tropical sea-surface temperatures continued increasing into the middle Frasnian starting with the base of the Rhinestreet IIc TR cycle (Joachimski and Buggisch, 1993; Joachimski et al, 2004), potentially exceeding 35°C. Dacryoconarids went extinct in tropical basins including the Appalachian Basin in the late Frasnian (Bond, 2006). Sea-surface temperature changes might, therefore, explain the long-term body-size trends in both embryonic and adult stages, as well as potentially account for the disappearance of the group in the basin.

Although the temperature size rule (Angiletta et al., 2004) is variable across species, temperature tends to reduce larval stage duration in both lecithotrophic and planktotrophic taxa due to faster growth rates (O'Connor et al., 2007). While there are contrasting predictions about how larval size affects duration due to species-specific contributions toward larval development, metabolic theory predicts that development time and adult body size should be positively correlated, which ((Fig. 8; Brown et al., 2004). Therefore, if starting small offered metabolic advantages in a warming environment, it is reasonable to infer that increased temperature led to reduced initial chamber size, as well as adult volume.

6. CONCLUSIONS

This study examined the diversity and body-size trends of late Givetian-middle Frasnian dacryoconarid assemblages in the northern Appalachian Basin. Dacryoconarid adult conch volumes gradually decrease up section from the Givetian-Frasnian boundary in a pattern suggesting evolution toward smaller volumes. Both adult and initial chamber volumes are statistically significantly smaller during the *punctata* positive carbon isotope excursion compared to background conditions.

Increased nutrient availability during the onset of the excursion in the early Frasnian is coincident with the largest adult volumes but a return to normal marine nutrient levels during the peak of the excursion suggests other factors are also responsible for significant size reductions. Taxonomic turnover only played a minor role in dacryoconarid size variability at each stratigraphic level. There is no evidence that bottom-water redox state contributed to size reductions, but frequent overturning of anoxic water masses during the early Frasnian may have favored thinner-shelled styliolinids over nowakiids, leading to lower generic diversity compared to the Givetian. There is better support for long-term warming to explain the gradual reduction in volumes through

the late Givetian and into the middle Frasnian. The relatively minor influence of the *punctata* excursion on dacryoconarid body size and turnover agrees with findings of studies on other invertebrate groups that suggest the event did not substantially affect biodiversity (Morrow et al., 2009). Altogether temperature offers the strongest correlate with dacryoconarid adult and initial chamber volume in the Appalachian Basin. The demonstrated relationship here, therefore, suggests that temperature could also explain global body-size trends of tentaculitoids during the Devonian Period.

ACKNOWLEDGEMENTS

This research was supported by a Syracuse University Department of Earth and Environmental Sciences Summer Research Grant to Prow-Fleischer and the National Science Foundaton Frontier Research in Earth Sciences grants # 2121445 to Lu., and #2121392 to Payne. We thank Lucy Weisbeck and Caroline Underwood for laboratory preparations. We also thank the editor, David E. Fastovsky, and two anonymous reviewers for their helpful critiques. We acknowledge that field collection was performed on the traditional land of the Haudenosaunee People.

APPENDIX I: SUPPLEMENTARY FIGURES

APPENDIX II: EXTENDED DISCUSSION

Potential Facies Control on Size Distributions

Changes in the style of preservation, especially those that are size-biased, can lead to a skewed view of diversity and abundance with implications for evolutionary trends in size traits or extinction selectivity (Payne,2005; Allison and Bottjer, 2010; Brown et al., 2022). A reduction in adult sizes begins in the early Frasnian in the North Evans Limestone. Because this is a lag deposit, the overall smaller shell sizes resulted from sorting, which would not have directly affected initial

chamber volumes (Fig. 3). Silicification, documented in the overlying Genundewa styliolinid grainstone, is taxonomic- and size-biased, favoring the preservation of smaller specimens (Pruss et al., 2015). While silicification may account for the low diversity and small volumes in this horizon, it cannot explain the gradual declining size trend through the early Frasnian or shift during the *punctata* excursion.

Taxonomic Composition

Three scenarios can, independently or combined, lead to the apparent trend toward smaller sizes between consecutive horizons: (1) size-biased extinction of larger-bodied taxa, (2) origination of smaller taxa, and (3) rapid size reduction in continuous lineages (Morten and Twitchett, 2009; Rego et al., 2012; Atkinson et al., 2019). Because nowakiid species are not unusually large (Fig. A4), their disappearance at the Givetian-Frasnian boundary and their stratum-specific origination in the basal West River Shale, do not cause any important overall changes between consecutive horizons. The small-sized species in the Genundewa Limestone between two barren horizons imposes a large disappearance effect followed by the origination size effect (Fig. 7). Even in these horizons with large among-lineage effects, the within-lineage size shifts are similar in magnitude and from the upper *transitans* through *punctata* biozones only within-lineage effects contribute to the observed size reductions. Therefore, dacryoconarid size shifts are more likely to have beendriven by evolutionary change in response to environmental factors rather than extinction or origination selectivity among lineages.

Nutrient Availability

In size-structured ecosystem models, increased nutrient supply stimulates larger phytoplankton biomass, which can support both a greater abundance and distribution of zooplankton size classes

(Fuchs and Franks, 2010). The organic-rich (TOC >1%) basal meter of both the Middlesex and Rhinestreet Formations are elevated in N and P above the Redfield ratio, indicating greater nutrient availability (Fig. S5). Increased nutrient availability supports the greater abundance of dacryoconarids along bedding planes. Furthermore, the largest adult volumes occur during Middlesex IIb TR cycle, coincident with the highest nutrient inventories, and suggests a causal relationship. Because of the tight coupling between TOC and nutrient supplyin the Middlesex and Rhinestreet Formations, the low TOC (<0.5%) content of the Cashaqua Formation suggests normal marine nutrient levels during the *punctata* excursion. A return to normal nutrient inventory cannot explain the shift in sizes after deposition of the Middlesex Formation.

Dacryoconarids are inferred to have lecithotrophic (non-feeding) larvae (Wei et al., 2012). Wei (2019) suggested that because dacryoconarids had lecithotrophic larvae with additional nutritional storage they were able to persist in the unfavorable conditions of the late Devonian until the late Frasnian, whereas tentaculitoids groups with planktotrophic larvae perished in the middle Frasnian. Studies on the modern bivalve *Nuculana acuta* from the Gulf of Mexico, which also has lecithotrophic larvae, show that larval size decreases with increasing eutrophication (Harnik et al., 2017). As nutrient levels increase, larvae require less nutrient storage capacity before reaching the conditions necessary to metamorphose into a feeding juvenile stage. However, this pattern is the opposite of what is observed in this study. High nutrient levels are associated with larger initial chamber sizes within the basal meter of the Middlesex and Rhinestreet Formations. Because of the relationship between the initial chamber and adult volumes, other factors must explain the coincident size decrease during the *punctata* excursion.

REFERENCES CITED

Aboussalam, Z.S., and Becker, R.T., 2011, The global Taghanic Biocrisis (Givetian) in the eastern Anti-Atlas, Morocco: Palaeogeography, Palaeoclimatology, Palaeoecology, v. 304, p. 136–164, https://doi.org/10.1016/j.palaeo.2010.10.015.

Algeo, T.J., and Lyons, T.W., 2006, Mo-total organic carbon covariation in modern anoxic marine environments: Implications for analysis of paleoredox and paleohydrographic conditions: Paleoceanography, v. 21, PA1016, https://doi.org/10.1029/2004PA001112.

Angilletta, M.J., Steury, T.D., and Sears, M.W., 2004, Temperature, growth rate, and body size in ectotherms: Fitting pieces of a life-history puzzle: Integrative and Comparative Biology, v. 44, p. 498–509, https://doi.org/10.1093/icb/44.6.498.

Atkinson, J., PB, Wignall., Morton, J., and Aze, T., 2019, Body size changes in bivalves of the family Limidae in the aftermath of the end - Triassic mass extinction: the Brobdingnag effect .: Palaeontology, v. 62, p. 561–582, https://doi.org/10.1111/pala.12415.

Baird, G.C., Kirchgasser, W.T., Over, J., and Brett, C.E., 2006, An early late Devonian bone bed-pelagic limestone succession: the North Evans-Genundewa Limestone story, *in* Jacobi,R.ed.,New York State Geological Association 78th Annual Meetingg Field Trips Guidebook:New York State Geological Association, p. 354–395.

Becker, R.T., Königshof, P., and Brett, C.E., 2016, Devonian climate, sea level and evolutionary events: An introduction, in Becker, R.T., Königshof, P., and Brett, C.E., eds., Devonian Climate, Sea Level and Evolutionary Events: Geological Society Special Publication, v. 423, p. 1–10, https://doi.org/10.1144/SP423.15.

Becker, R.T., Marshall, J.E.A., Da Silva, A.-C., Agterberg, F.P., Gradstein, F.M., and Ogg, J.G., 2020, The Devonian Period, *in* Gradstein, F.M., Ogg, J.G., Schmitz, M.D., and Ogg, G.M., eds.,

Geologic Time Scale 2020: Amsterdam, Elsevier,p. 733–810, https://doi.org/10.1016/b978-0-12-824360-2.00022-x.

Bond, D., 2006, The fate of the homoctenids (Tentaculitoidea) during the Frasnian-Famennian mass extinction (Late Devonian): Geobiology, v. 4, p. 167–177, https://doi.org/10.1111/j.1472-4669.2006.00078.x.

Bouček, B., 1964, The Tentaculites of Bohemia: Their Morphology, Taxonomy, Ecology, Phylogeny and Biostratigraphy (): Prague, Publishing House of the Czechoslovak Academy of Sciences. [M.L. Dutkova, translator]

Brett, C.E., 1974, Biostratigraphy and paleoecology of the Windom Shale Member (Moscow Formation) in Erie County, NY, *in* Peterson, D.N., ed., Annual Meeting of the New York State Geological Association 46th Annual Meeting Field Trip Guidebook: New York State Geological Association, p. G1-G15.

Brocke, R., Fatka, O., Lindemann, R.H., Schindler, E., and Straeten, C.A.V.E.R., 2016, Palynology, dacryoconarids and the lower Eifelian Event (Middle Devonian) Basal Choteč Event: case studies from the Prague and Appalachian basins, in Becker, R. T., Königshof, P. & Brett, C.E. ed., Devonian Climate, Sea Level and Evolutionary Events., The Geological Society of London., p. 123–169, http://doi.org/10.1144/SP423.8.

Brown, C.M., Campione, N.E., Wilson Mantilla, G.P., and Evans, D.C., 2022, Size-driven preservational and macroecological biases in the latest Maastrichtian terrestrial vertebrate assemblages of North America: Paleobiology, v. 48, p. 210–238, https://doi.org/10.1017/pab.2021.35.

Cereja, R., 2020, Critical thermal maxima in aquatic ectotherms: Ecological Indicators, v. 119,,

https://doi.org10.1016/j.ecolind.2020.106856.

Deutsch, C., Penn, J.L., Verberk, W.C.E.P., and Inomura, K., Endress, M.-G., and Payne, J.L., 2022, Impact of warming on aquatic body sizes explained by metabolic scaling from microbes to macrofauna: PNAS, v. 119, https://doi.org/10.1073/pnas.2201345119.

Farsan, N.M., 2005, Description of the early ontogenic part of the Tentaculitids, with implications for classification: Lethaia, v. 38, p. 255–270, https://doi.org10.1080/00241160510013349.

Ferreira, T., and Rasband, W.,2012, ImageJ User Guide:, https://imagej.net/ij/ij/docs/guide/index.html.[Accessed August 8, 2023].

Fuchs, H., and Franks, P., 2010, Plankton community properties determined by nutrients and size-selective feeding: Marine Ecology Progress Series, v. 413, p. 1–15, https://doi.org/10.3354/meps08716.

Gaston, K.J., and Blackburn, T.M., 1996, Range Size-Body Size Relationships: Evidence of Scale Dependence: Oikos, v. 75, p. 479-485, https://doi.org10.2307/3545889.

Gillooly, J.F., Brown, J.H., West, G.B., Savage, V.M., and Charnov, E.L., 2001, Effects of size and temperature on metabolic rate: Science, v. 293, p. 2248–2251, https://doi.org/10.1126/science.1061967 .

Grabau, A.W., 1898, Geology and Paleontology of Eighteen Mile Creek and the Lake Shore Sections of Erie County, New York: Buffalo Society of Natural Sciences, Buffalo, p. -401

Hammer, Ø., and Harper, D.A.T. (Eds.), 2005, Paleontological Data Analysis: Wiley-Blackwell, p. 81-94.

Hansen, T.F., 1997, Stabilizing selection and the comparative analysis of adaptation: Evolution, v.

51, p. 1341–1351, https://doi.org10.1111/j.1558-5646.1997.tb01457.x.

Harnik, P.G., Torstenson, M.L., and Williams, M.A., 2017, Assessing the effects of anthropogenic eutrophication on marine bivalve life history in the northern Gulf of Mexico: PALAIOS, v. 32, p. 678–688, https://doi.org10.2110/palo.2017.033.

Hunt, G., 2022, Basics of paleoTS: https://cran.r-project.org/web/packages/paleoTS/vignettes/paleoTS_basics.html. [Accessed January 10, 2024].

Hunt, G., 2007, The relative importance of directional change, random walks, and stasis in the evolution of fossil lineages: Proceedings of the National Academy of Sciences of the United States of America, v. 104, p. 18404–18408, https://doi.org/10.1073/pnas.1403662111.

Hunt, G., Hopkins, M.J., and Lidgard, S., 2015, Simple versus complex models of trait evolution and stasis as a response to environmental change: Proceedings of the National Academy of Sciences of the United States of America, v. 112, p. 4885–4890, doi:10.1073/pnas.1403662111.

Jimenez, M.Y., Ivany, L.C., Judd, E.J., and Henkes, G., 2019, Low and seasonally variable salinity in the Pennsylvanian equatorial Appalachian Basin: Earth and Planetary Science Letters, v. 519, p. 182–191, https://doi.org/10.1016/j.epsl.2019.04.051.

Joachimski, M.M., and Buggisch, W., 1993, Anoxic events in the late Frasnian - causes of the Frasnian- Famennian faunal crisis?: Geology, v. 21, p. 675–678, https://doi.org/10.1130/0091-7613(1993)0212.3.CO;2.

Joachimski, M.M., Van Geldern, R., Breisig, S., Buggisch, W., and Day, J., 2004, Oxygen isotope evolution of biogenic calcite and apatite during the Middle and Late Devonian: International Journal of Earth Sciences, v. 93, p. 542–553, https://doi.org10.1007/s00531-004-0405-8.

Joachimski, M.M., Breisig, S., Buggisch, W., Talent, J.A., Mawson, R., Gereke, M., Morrow, J.R., Day, J., and Weddige, K., 2009, Devonian climate and reef evolution: Insights from oxygen isotopes in apatite: Earth and Planetary Science Letters, v. 284, p. 599–609, https://doi.org/10.1016/j.epsl.2009.05.028.

Johnson, J.G., Klapper, G., and Sandberg, C.A., 1985, Devonian eustatic fluctuations in Euramerica.: Geological Society of America Bulletin, v. 96, p. 567–587, https://doi.org/10.1130/0016-7606(1985)962.0.CO;2. Judd, E.J., Bhattacharya, T., and Ivany, L.C., 2020, A Dynamical Framework for Interpreting Ancient Sea Surface Temperatures: Geophysical Research Letters, v. 47, https://doi.org/10.1029/2020GL089044Kaufmann, B., 2006, Calibrating the Devonian Time Scale: A synthesis of U–Pb ID–TIMS ages and conodont stratigraphy: Earth-Science Reviews, v. 76, p. 175–190, https://doi.org/10.1016/j.earscirev.2006.01.001.

Klapper, G., and Kirchgasser, W.T., 2016, Frasnian Late Devonian conodont biostratigraphy in New York: graphic correlation and taxonomy: Journal of Paleontology, v. 90, p. 525–554, https://doi.org/10.1017/jpa.2015.70.

Larsson, 1979, Silurian tentaculitids from Gotland and Scania : Oslo, Universitetsforlaget, Fossils and Strata, v. 5, p. 1-180

Lash, G.G., 2019, A global biogeochemical perturbation during the Middle Frasnian punctata Event: Evidence from muted carbon isotope signature in the Appalachian Basin, New York State (USA): Global and Planetary Change, v. 177, p. 239–254, https://doi.org/10.1016/j.gloplacha.2019.01.006.

Lindemann, R.H., and Yochelson, E.L., 1984, Styliolines from the Onondaga Limestone (Middle

Devonian) of New York.: Journal of Paleontology, v. 58, p. 1251–1259.

Meehan, K.C., and Boyle, J.T., 2021, Marine Crisis Events and Fossils of the Late Devonian Appalachian Basin Deltaic Sequence of Western New York, in n Solar, G.S., and Valentino, D.W., eds., New York State Geological Association 92nd Annual Conference Field Guide, p. 1–26.

Meiri, S., and Dayan, T., 2003, On the validity of Bergmann's rule: Journal of Biogeography, v. 30, p. 331–351, https://doi.org/10.1046/j.1365-2699.2003.00837.x.

Montañez, I.P., Osleger, D.J., Chen, J., Wortham, B.E., Stamm, R.G., Nemyrovska, T.I., Griffin, J.M., Poletaev, V.I., and Wardlaw, B.R., 2018, Carboniferous climate teleconnections archived in coupled bioapatite δ 18 O PO 4 and 87Sr/86Sr records from the epicontinental Donets Basin, Ukraine: Earth and Planetary Science Letters, v. 492, p. 89–101, https://doi.org/10.1016/j.epsl.2018.03.051. Morrow, J.R., Sandberg, C.A., Malkowski, K., and Joachimski, M.M., 2009, Carbon isotope chemostratigraphy and precise dating of middle Frasnian (lower Upper Devonian) Alamo Breccia, Nevada, USA: Palaeogeography, Palaeoclimatology, Palaeoecology, v. 282, p. 105–118, https://doi.org/10.1016/j.palaeo.2009.08.016.

Morten, S.D., and Twitchett, R.J., 2009, Fluctuations in the body size of marine invertebrates through the Pliensbachian-Toarcian extinction event: Palaeogeography, Palaeoclimatology, Palaeoecology, v. 284, p. 29–38, https://doi.org/10.1016/j.palaeo.2009.08.023.

Murphy, A.E., Sageman, B.B., and Hollander, D.J., 2000, Eutrophication by decoupling of the marine biogeochemical cycles of C, N, and P: A mechanism for the Late Devonian mass extinction: Geology, v. 28, p. 427–430, https://doi.org/10.1130/0091- 691

7613(2000)282.0.CO;2. https://doi.org10.1130/0091-7613.

O'Connor, M.I., Bruno, J.F., Gaines, S.D., Halpern, B.S., Lester, S.E., Kinlan, B.P., and Weiss, J.M., 2007, Temperature control of larval dispersal and the implications for marine ecology, evolution, and conservation: Proceedings of the National Academy of Sciences, v. 104, p. 1266–1271, https://doi.org/10.1073/pnas.0603422104.Origin(Pro), Version Number 2024. OriginLab Corporation, Northampton, MA, USA.

Over, D., Baird, G., and Kirchgasser, W.T., 2023, Chapter 8: The Frasnian strata—Lower Upper Devonian—of New York State, in Ver Straeten, C., Over, J.D., and Woodrow, D. eds., Devonian of New York, Volume 3: Frasnian to Famennian (Upper Devonian) stages and the Devonian terrestrial system in New York, Bulletins of American Paleontologyy, v. 407–408, p. 1–28, https://doi.org/10.32857/bap.2023.407.01.

Payne, J.L., 2005, Evolutionary dynamics of gastropod size across the end-Permian extinction and through the Triassic recovery interval: Paleobiology, v. 31, p. 269–290, https://doi.org/10.1666/0094-8373(2005)031[0269:EDOGSA]2.0.CO;2.

Payne, J.L., and Heim, N.A., 2020, Body size, sampling completeness, and extinction risk in the marine fossil record: Paleobiology, v. 46, p. 23–40,https://doi.org/10.1017/pab.2019.43.Pisarzowska, A., and Racki, G., 2012, Isotopic chemostratigraphy across the Early–Middle Frasnian transition (Late Devonian) on the South Polish carbonate shelf: A reference for the global punctata Event: Chemical Geology, v. 334, p. 199–220, https://doi.org/10.1016/j.chemgeo.2012.10.034. Pisarzowska, A., Becker, R.T., Aboussalam, Z.S., Szczerba, M., Sobień, K., Kremer, B., Owocki, K., and Racki, G., 2020, Middlesex/punctata Event in the Rhenish Basin (Padberg section, Sauerland, Germany) –

Geochemical clues to the early-middle Frasnian perturbation of global carbon cycle: Global and Planetary Change, v. 191, https://doi.org/10.1016/j.gloplacha.2020.103211.Prow, A.N., Lu, Z., Frappier, A.B., Weisbeck, L.E., and Underwood, C.R., 2023, Extraction of calcareous dacryoconarid microfossils from limestones and mudrocks by surfactants paired with freeze-thaw processing: Marine Micropaleontology, v. 180, https://doi.org/10.1016/j.marmicro.2023.102216

Pucéat, E. et al., 2010, Revised phosphate–water fractionation equation reassessing paleotemperatures derived from biogenic apatite: Earth and Planetary Science Letters, v. 298, p. 135–142, doi:10.1016/j.epsl.2010.07.034.

Pruss, S.B., Payne, J.L., and Westacott, S., 2015, Taphonomic bias of selective silicification revealed by paired petrographic and insoluble residue analysis: PALAIOS, v. 30, p. 620–626, doi:10.2110/palo.2014.105 https://doi.org/10.1016/j.epsl.2010.07.034.Redfield, A.C., Ketchum, B.H., and Richards, F.A., 1963, The influence of organisms on the composition of seawater, *in* Hill, ed., The sea, Volume 2: New York, Interscience Press, p. 26–77.

Rego, B.L., Wang, S.C., Altiner, D., and Payne, J.L., 2012, Within- and among-genus components of size evolution during mass extinction, recovery, and background intervals : a case study of Late Permian through Late Triassic foraminifera: v. 38, p. 627–643.

Retallack, G.J., and Huang, C., 2011, Ecology and evolution of Devonian trees in New York, USA: Palaeogeography, Palaeoclimatology, Palaeoecology, v. 299, p. 110–128, https://doi.org/10.1666/11040.1.

Rita, P., Nätscher, P., Duarte, L.V., Weis, R., and De Baets, K., 2019, Mechanisms and drivers of belemnite body-size dynamics across the Pliensbachian-Toarcian crisis: Royal Society Open

Science, v. 6, https://doi.org/10.1098/rsos.190494.

Sageman, B.B., Murphy, A.E., Werne, J.P., Ver Straeten, C.A., Hollander, D.J., and Lyons, T.W., 2003, A tale of shales: The relative roles of production, decomposition, and dilution in the accumulation of organic-rich strata, Middle-Upper Devonian, Appalachian basin: Chemical Geology, v. 195, p. 229–273, , https://doi.org/10.1016/S0009-2541(02)00397-2.

Schindler, E., 2012, Tentaculitoids—An enigmatic group of Palaeozoic fossils, in Talent, J.A., ed., Earth and Life: Global Biodiversity, Extinction Intervals and Biogeographic Perturbations Through Time: Dordrecht, Springer, p. 479–490, https://doi.org/10.1007/978- 743 90-481-3428-1_14.Schöne, B.R., 1999, Scleroecology: Implications for ecotypical dwarfism in oxygen-restricted environments (Middle Devonian, Rheinisches Schiefergebirge): Senckenbergiana lethaea, v. 79, p. 35–41, https://doi.org/10.1007/BF03043212.

Scotese, C.R., 2014, Atlas of Devonian Paleogeographic Maps, *in* PALEOMAP Atlas for ArcGIS, volume 4, The Late Paleozoic, Maps 65-72, Mollweide Projection, PALEOMAP Project, Evanston, IL.: Paleo, http://rgdoi.net/10.13140/2.1.1542.5280 (accessed May 2024).

Scotese, C.R., and McKerrow, W.S., 1990, Revised World maps and introduction, in McKerrow, W.S., and Scotese, C.R., eds., Palaeozoic Palaeogeography and Biogeography:: Geological Society, London, Memoirs, v. 12, p. 1–21, https://doi.org/10.1144/GSL.MEM.1990.012.01.01

Sibly, R.M., and Atkinson, D., 1994, How Rearing Temperature Affects Optimal Adult Size in Ectotherms: Functional Ecology, v. 8, p. 486-493,https://doi.org/10.2307/2390073..

Vance, R.R., 1973, On Reproductive Strategies in Marine Benthic Invertebrates: The American Naturalist, v. 107, p. 339–352, https://doi.org/10.1086/282838

Ver Straeten, C., 2023, Chapter 1. An introduction to the Devonian period, and the Devonian in

New York state and North America, in Ver Straeten, C., Over, J.D., and Woodrow, D. eds., Devonian of New York, Volume 1: Introduction and Přídolí to lower Givetian (Upper Silurian to Middle Devonian) stagess: Bulletins of American Paleontology, v. 403–404, p. 11–102, 762 https://doi.org/10.32857/bap.2023.403.03, Wei, F., 2019, Conch size evolution of Silurian–Devonian tentaculitoids: Lethaia, v. 52, p. 454–463, https://doi.org/10.1111/let.12324.

Wei, F., Gong, Y., and Yang, H., 2012, Biogeography, ecology and extinction of Silurian and Devonian tentaculitoids: Palaeogeography, Palaeoclimatology, Palaeoecology, v. 358–360, p. 40–50, https://doi.org10.1016/j.palaeo.2012.07.019.

Wilson, A.B., 2009, Fecundity selection predicts Bergmann's rule in syngnathid fishes: Molecular Ecology, v. 18, p. 1263–1272, https://doi,org10.1111/j.1365-294X.2009.04084.x.

Wittmer, J.M., and Miller, A.I., 2011, Dissecting the global diversity trajectory of an enigmatic group: The paleogeographic history of tentaculitoids: Palaeogeography, Palaeoclimatology, Palaeoecology, v. 312, p. 54–65, https://doi.org/10.1016/j.palaeo.2011.09.009.

Yamaguchi, T., Norris, R.D., and Bornemann, A., 2012, Dwarfing of ostracodes during the Paleocene – Eocene Thermal Maximum at DSDP Site 401 (Bay of Biscay , North Atlantic) and its implication for changes in organic carbon cycle in deep-sea benthic ecosystem: Palaeogeography, Palaeoclimatology, Palaeoecology, v. 346–347, p. 130–144, https://doi.org10.1016/j.palaeo.2012.06.004.

Yans, J., Corfield, R.M., Racki, G., and Preat, A., 2007, Evidence for perturbation of the carbon cycle in the Middle Frasnian punctata Zone (Late Devonian): Geological Magazine, v. 144, p. 263–270, https://doi.org/10.1017/S0016756806003037.

Yochelson, E.L., and Kirchgasser, W.T., 1986, The Youngest Styliolines and Nowakiids (Late

Devonian) Currently Known from New York: Journal of Paleontology, v. 60, p. 689–700. https://doi.org/10.1017/S0022336000022216.

Zambito, J.J., IV,Joachimski, M.M., Brett, C.E., Baird, G.C., and Aboussalam, Z.S., 2016, A carbonate carbon isotope record for the late Givetian (Middle Devonian) Global Taghanic Biocrisis in the type region (northern Appalachian Basin), *in* n Becker, R.T., Königshof, P., and Brett, C.E., eds., Devonian Climate, Sea Level and Evolutionary Events., London, Special Publication 423, p. 223–233, https://doi.org/10.1144/SP423.7.**FIGURE CAPTIONS**

Figure 1: Dacryoconarid morphology. (A) Diagram of morphological characteristics of dacryoconarids indicting divisions between growth stages (Larsson, 1979; Wei et al., 2012)**.**(B) Features of external structure that distinguish common genera (Bouček, 1964). Dashed features indicate features that may or may not be present, and lighter gray lines indicate features that are fainter and may require scanning electron microscopy to observe. (C) variety in embryonic chamber shape with approximate scale (Farsan, 2005).

Figure 2: Map of study area. (A) Map of Erie County in Western New York (USA). Stars are localities that correspond to stops detailed in Meehan & Boyle (2021) and compose the composite stratigraphic section under study. Sites are named after nearby geographical identifiers along Eighteen Mile Creek as follows: A - Basswood Drive North Side (42.7077° N, 78.9562° W); B - Basswood Drive South Side (42.7077° N, 78.9561° W); C - Hobuck Flats (42.7077° N, 78.9561° W); D - North Evans Cemetery (42.6950° N, 78.9362° W); E - Preischel Farm (42.6836° N, 78.8798° W). The red oval is the approximate location of the study site from Lash (2019). Inset map of New York State shows locations of study area and Akzo core from which geochemical data used in this study was measured by Sageman et al. (2003) (B) Paleogeographic map of Frasnian Age

showing study area (star) (Scotese, 2014), (C) Exposure of the contact between Cashaqua and Rhinestreet Formations at Site C with people for scale. Black dots in Cashaqua Formation represent carbonate concretions. Horizontal dashed represent shale lithology and the color gradient in the Cashaqua Formations represents a transition to more organic-rich sediment.

Figure 3: Stratigraphic trends in assemblage-scale dacryoconarid adult and initial chamber volumes at Eighteen Mile Creek. The horizontal axis on the stratigraphic column indicates the average grain size ranging from shale andvery fine-grained siltstone (v) to fine- (f), medium- (m) and coarse-grained (c) siltstone. The dashed line between the *hassi* biozone and overlying strata indicates uncertainty in boundary placement and identity of the overlying biozone. Greyscale gradients indicate relative changes in lithologic colordue to organic content. Dacryoconarid symbols to the right of the composite stratigraphic column indicate occurrences. The number inside represents the relative proportion on a scale of 1 to 5 of the abundance of dacryoconarids in the the sediment, where a 5 represents rock-forming quantities and a 1 indicates rarity. The gray band indicates the duration of *punctata* excursion and the dashed lines indicate unconformities. Arrows in size plots highlight the direction of the trend. Error bars are 1 standard deviation. Organic carbon isotope ($\delta^{13}C_{org}$) values, Mo concentrations, and percent total organic carbon (TOC) are from Lash (2019). Dashed vertical lines delineating modern anoxic basin [Mo]/TOC ratios from Algeo and Lyons (2006). Euramerican relative sea level curve modified from Johnson et al. (1985) where numerals refer to transgressive-regressive cycles.

Figure 4: (A) Nowakiid steinkern, Windom Shale, light microscope (B-C) Styliolinids from Cashaqua Formation, light microscope (D) stratum-specific occurrence of nowakiid, West

River Shale, light microscope (E, F) light and scanning electron photomicrographs of *Striatostlyiolina* sp. (G) scanning electron photomicrograph of silicified styliolinid, Genundewa Limestone.

Figure 5: Evolutionary trajectory modeling plots of mean log-transformed adult volume at each sampled stratigraphic interval. Vertical error bars are log-transformed variance. Gray bands are 95% confidence intervals. The Genundewa Limestone point is included on the plot but excluded from analyses due to inferred preservational bias (see Appendix: Extended Discussion). Vertical dashed lines indicate unconformities of unknown duration.

Figure 6: Stratigraphic trends in family relative abundance of assemblage at each horizon where n is the number of specimens measured at interval. Gray bars indicate no occurrences. Stratigraphic column not to scale. Dashed horizontal lines indicate unconformities. N.E. = North Evans Limestone; M.S. = Middlesex Formation; G.L.= Genundewa Limestone. Colored vertical bars correspond to lithology in figure 3.

Figure 7: Family-level within- and among-lineage components of size shifts for each consecutive bed. The total size shift of the assemblage between each bed and its previous consecutive bed in light blue is divided into the proportions attributable to within-lineage size change (dark blue), origination of new family between beds (yellow) and the disappearance of family between beds (orange). Gray band is *punctata* excursion. Dashed line represents Givetian-Frasnian boundary.

Figure 8: Covariation in log-transformed mean assemblage adult and initial chamber volumes for each conodont biozone colored by (A) average Mo/TOC ratio (TOC—total organic carbon) as a measure of basin restriction and (B) average Mo concentration as a measure of the

degree of bottom water anoxia (Lash, 2019). The slope of the linear regression is statistically significant from zero at a significant level ($\alpha = 0.05$).

Figure 9: Relationship between sea surface temperature and adult volume. (A) Late Devonian sea-surface temperature reconstruction using oxygen isotope ratios from conodont apatite ($\delta^{18}O_{apatite}$) data from Joachimski et al. (2004), the revised phosphate-water oxygen fractionation equation from (Pucéat et al., 2010) and a Devonian seawater value of -1 ‰. Dashed orange line is linear fit for temperature reconstruction (B) log-scaled assemblage (dotted line) and genus *Styliolina* (dark blue squares) adult volume. Dashed blue line linear fit for log-scaled *Styliolina* volumes (Pearson's r = -0.63, p = 0.004). Black horizontal dashed line represents unconformity spanning Givetian-Frasnian boundary. Horizontal grey and beige bands show the correspondence of vertical age between panels.

APPENDIX I: FIGURE CAPTIONS

Figure S1: Log-transformed adult volume distributions for each sampled interval.

Figure S2: Log-transformed initial chamber volume distributions for each sampled bed. Colored according to biozone with the "core" punctata referring to the middle of the positive excursion.

Figure S3: Evolutionary trajectory modeling. Plot of mean log-transformed initial chamber volume at each sampled stratigraphic interval. Vertical error bars indicate variance.

Figure S4: Family-level stratigraphic trends in mean log-transformed initial chamber volumes (A),

adult volumes (B), andadult to initial chamber volume ratio (C).

Figure S5: Geochemical proxy data for nutrient availability (A-C) and redox conditions (D-E) relevant to the interval spanning the upper West River Formation through the *punctata* zonation of the lower Rhinestreet Formation from the Akzo core #9455 (Sageman et al., 2003). Dashed horizontal line highlights this study's sampling gap. Vertical dotted lines are "gray shale mean" values used to denote normal, oxygenated marine values specific to the Appalachian Basin.

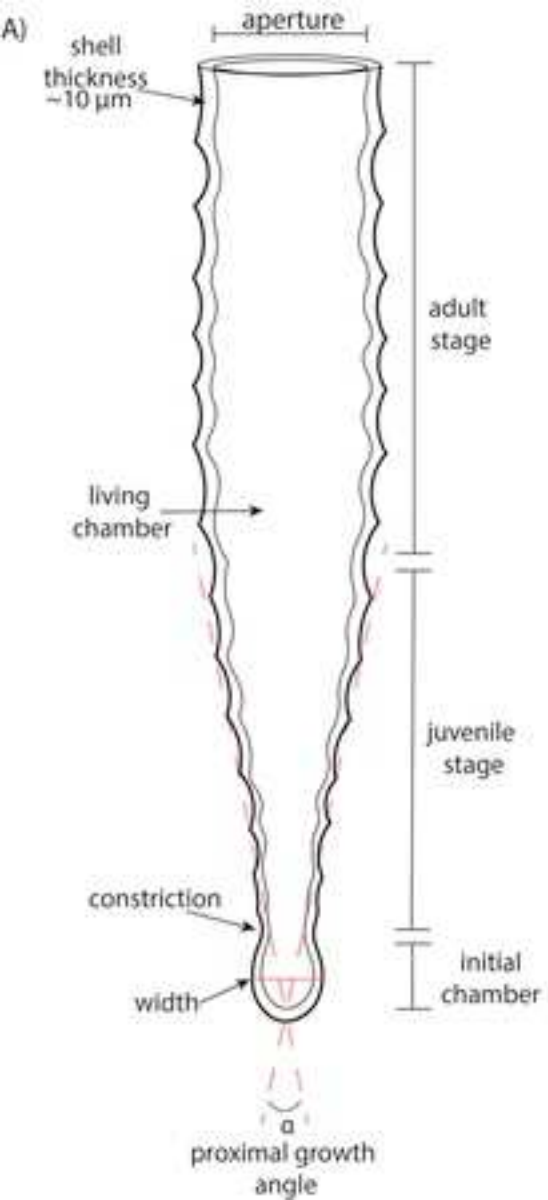
A)
aperture
shell thickness ~10 µm
adult stage
living chamber
juvenile stage
constriction
width
initial chamber
α
proximal growth angle

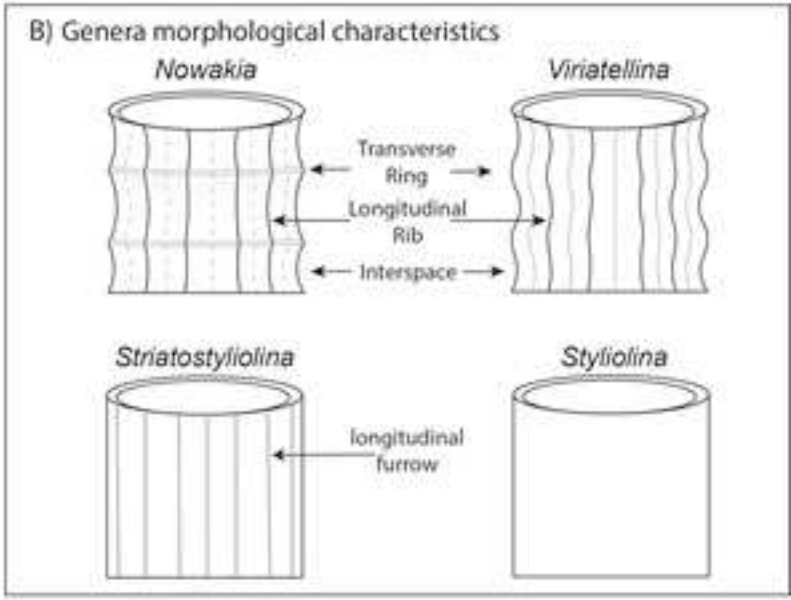
B) Genera morphological characteristics
Nowakia
Viriatellina
Transverse Ring
Longitudinal Rib
Interspace
Striatostyliolina
Styliolina
longitudinal furrow

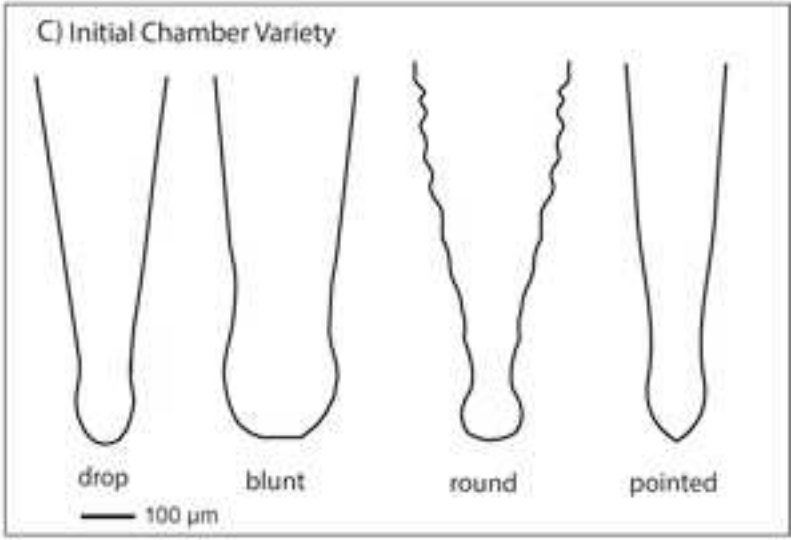
C) Initial Chamber Variety
drop
blunt
round
pointed
100 µm

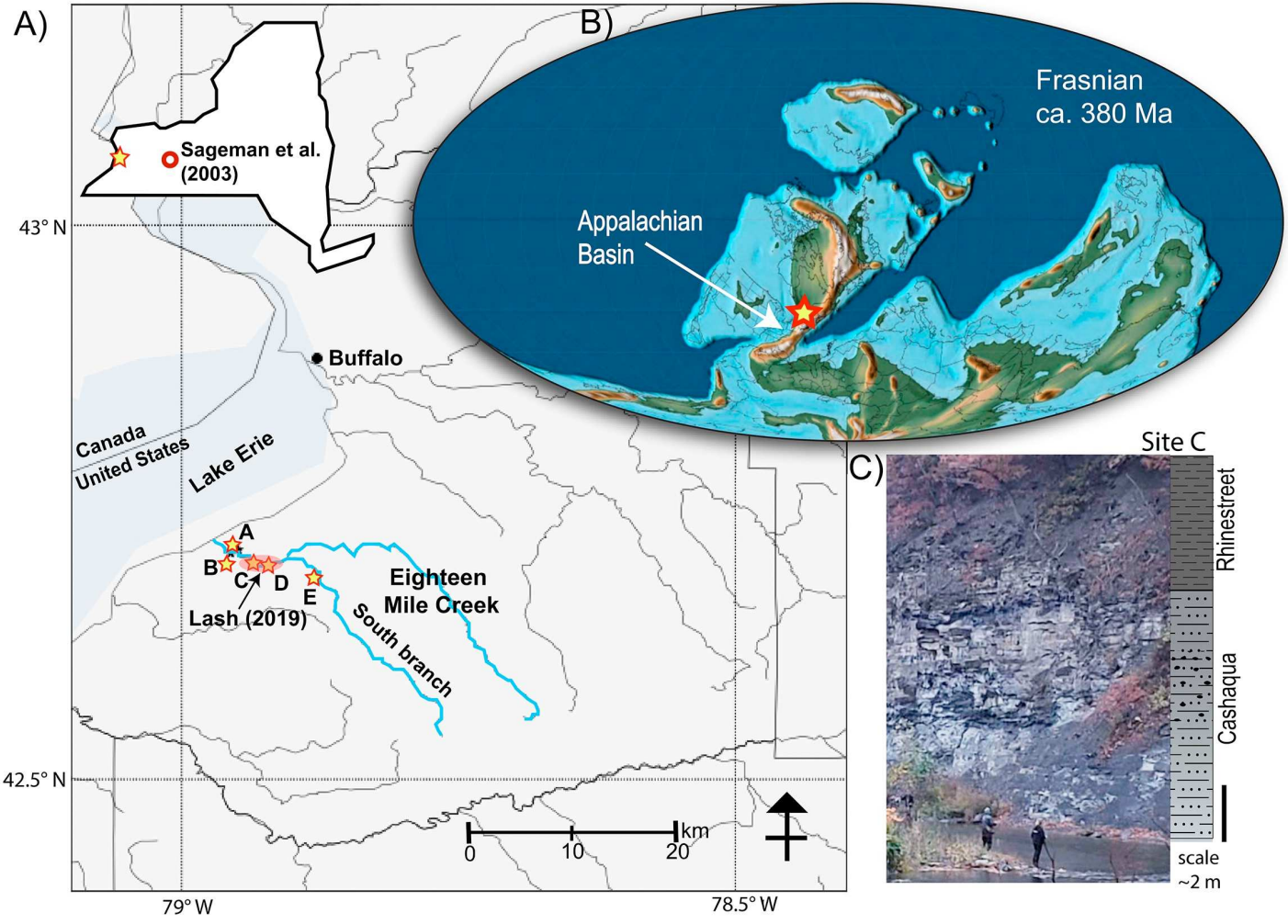
A)
B)
C)
Sageman et al. (2003)
43° N
42.5° N
79° W
78.5° W
Buffalo
Canada
United States
Lake Erie
A
B
C
D
E
Lash (2019)
Eighteen Mile Creek
South branch
0
10
20
km
Frasnian
ca. 380 Ma
Appalachian Basin
Site C
Rhinestreet
Cashaqua
scale ~2 m

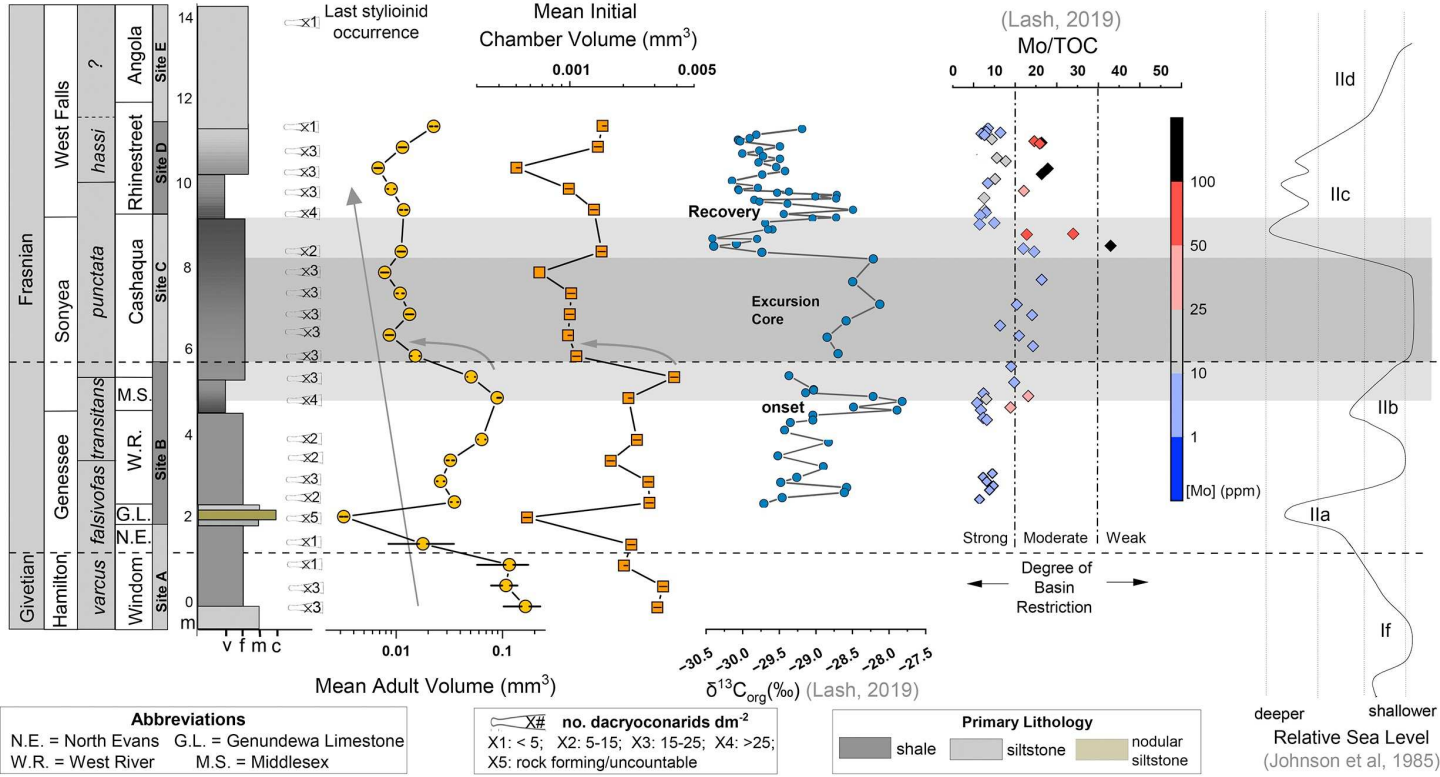
Frasnian
Givetian
West Falls
Sonyea
Genessee
Hamilton
?
hassi
punctata
transitans
falsivofas
varcus
Angola
Rhinestreet
Cashaqua
M.S.
W.R.
G.L.
N.E.
Windom
Site E
Site D
Site C
Site B
Site A
Last stylioinid occurrence
Mean Initial Chamber Volume (mm³)
0.001
0.005
Recovery
Excursion Core
onset
(Lash, 2019)
Mo/TOC
0 10 20 30 40 50
100
50
25
10
1
[Mo] (ppm)
Strong
Moderate
Weak
Degree of Basin Restriction
IId
IIc
IIb
IIa
If
deeper
shallower
Relative Sea Level
(Johnson et al, 1985)
v f m c
0.01
0.1
Mean Adult Volume (mm³)
-30.5 -30.0 -29.5 -29.0 -28.5 -28.0 -27.5
δ13Corg(‰) (Lash, 2019)
Abbreviations
N.E. = North Evans G.L. = Genundewa Limestone
W.R. = West River M.S. = Middlesex
no. dacryoconarids dm-2
X1: < 5; X2: 5-15; X3: 15-25; X4: >25;
X5: rock forming/uncountable
Primary Lithology
shale
siltstone
nodular siltstone

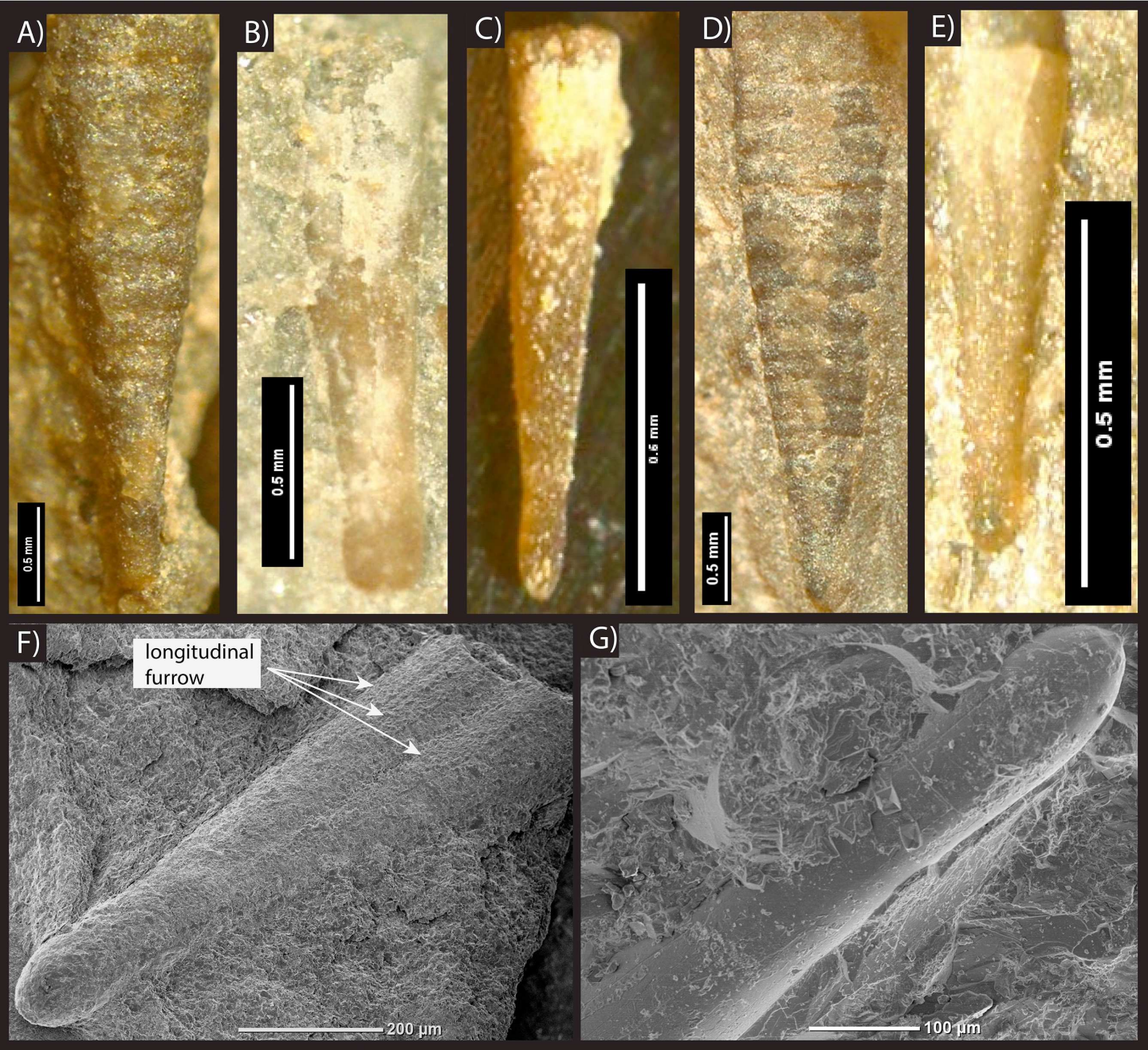
A)
0.5 mm
B)
0.5 mm
C)
0.5 mm
D)
0.5 mm
E)
0.5 mm
F)
longitudinal
furrow
200 µm
G)
100 µm

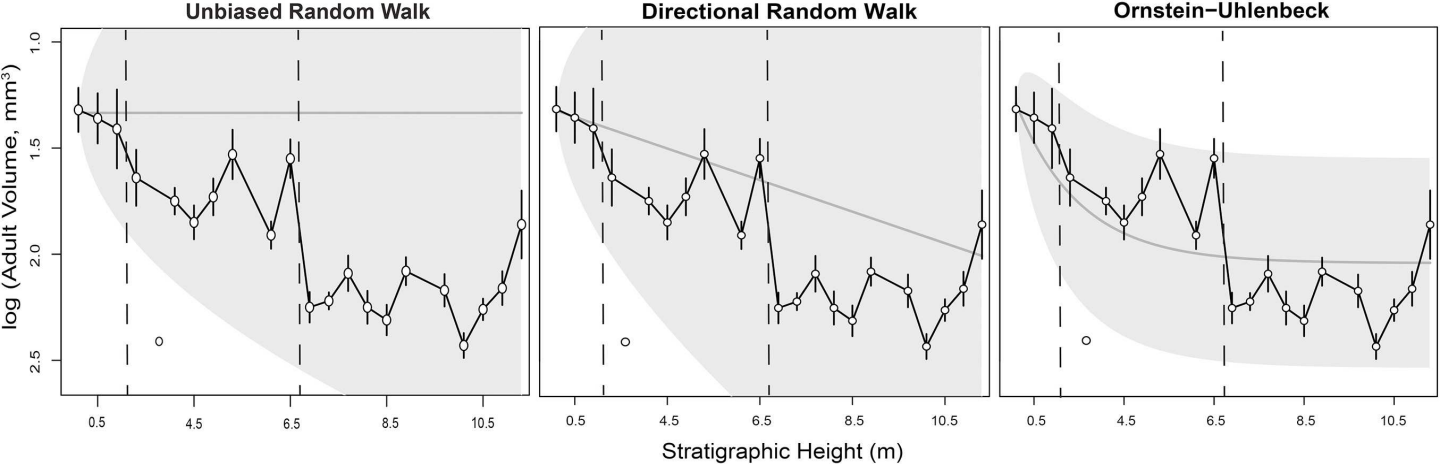
Unbiased Random Walk
Directional Random Walk
Ornstein−Uhlenbeck
log (Adult Volume, mm³)
1.0
1.5
2.0
2.5
0.5
4.5
6.5
8.5
10.5
Stratigraphic Height (m)

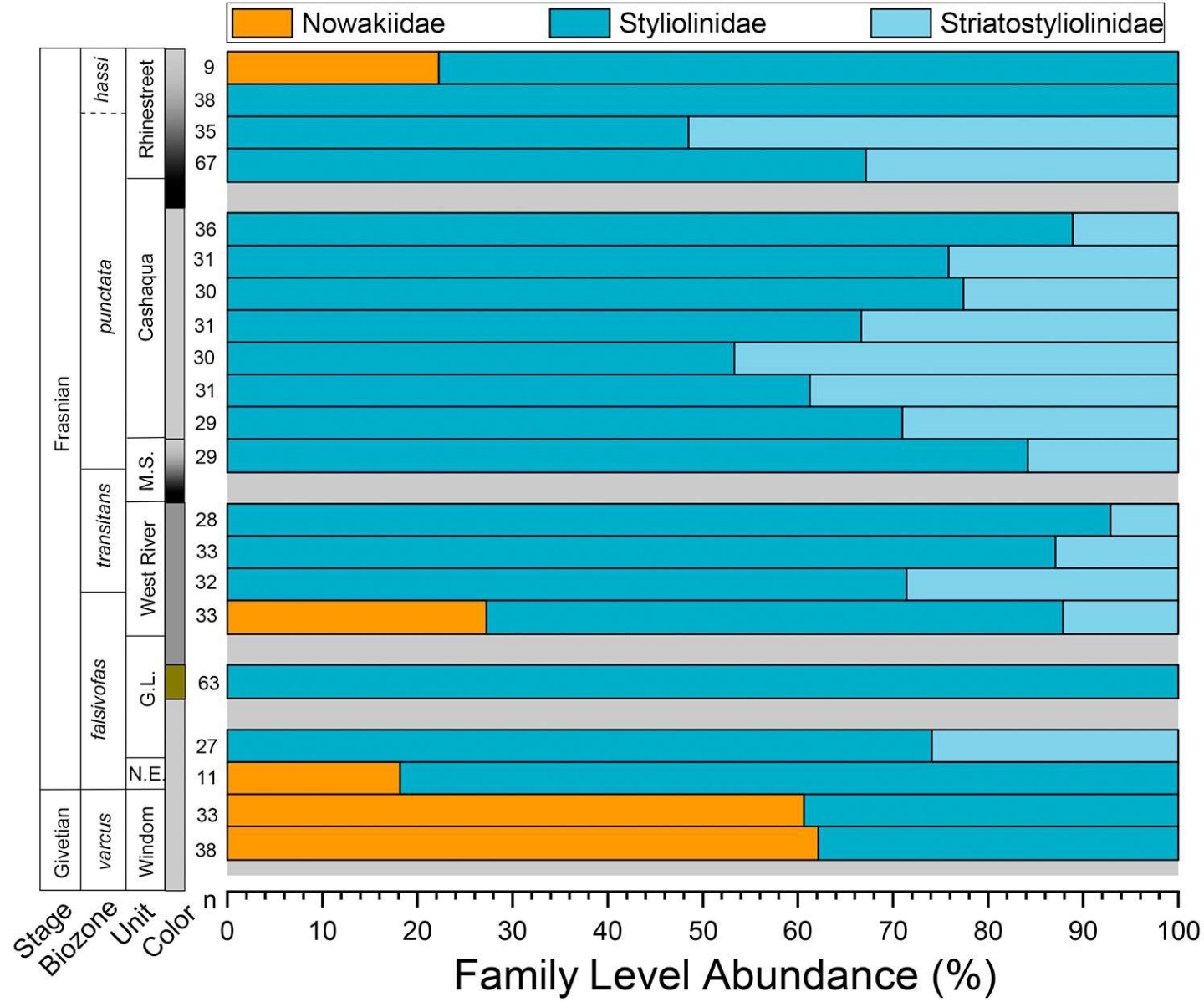
Nowakiidae
Styliolinidae
Striatostyliolinidae
Frasnian
Givetian
hassi
punctata
transitans
falsivofas
varcus
Rhinestreet
Cashaqua
M.S.
West River
G.L.
N.E.
Windom
9
38
35
67
36
31
30
31
30
31
29
29
28
33
32
33
63
27
11
33
38
n
Stage
Biozone
Unit
Color
0
10
20
30
40
50
60
70
80
90
100
Family Level Abundance (%)

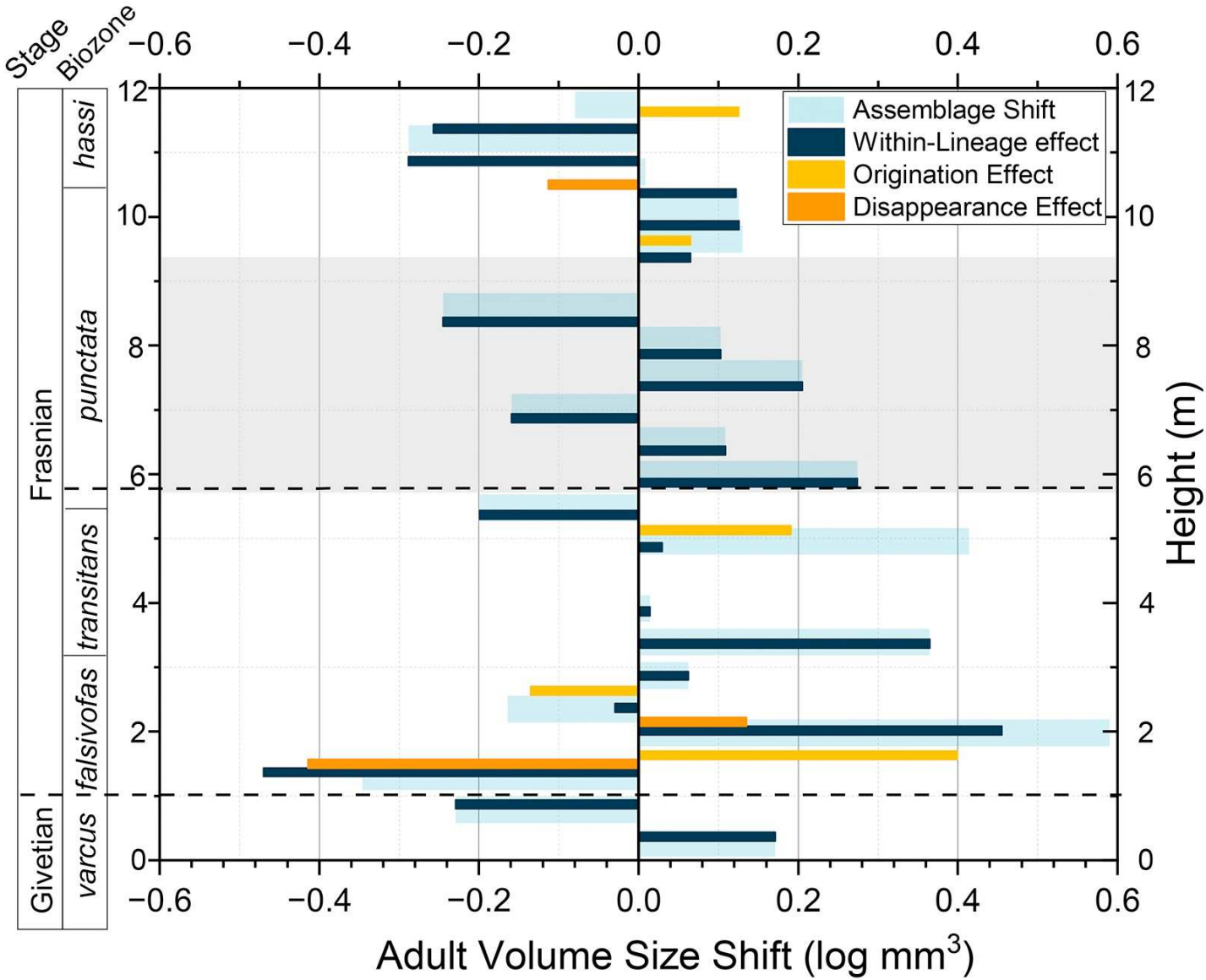
Stage
Biozone
Frasnian
Givetian
hassi
punctata
transitans
falsivofas
varcus
Assemblage Shift
Within-Lineage effect
Origination Effect
Disappearance Effect
Height (m)
Adult Volume Size Shift (log mm3)
−0.6
−0.4
−0.2
0.0
0.2
0.4
0.6
0
2
4
6
8
10
12

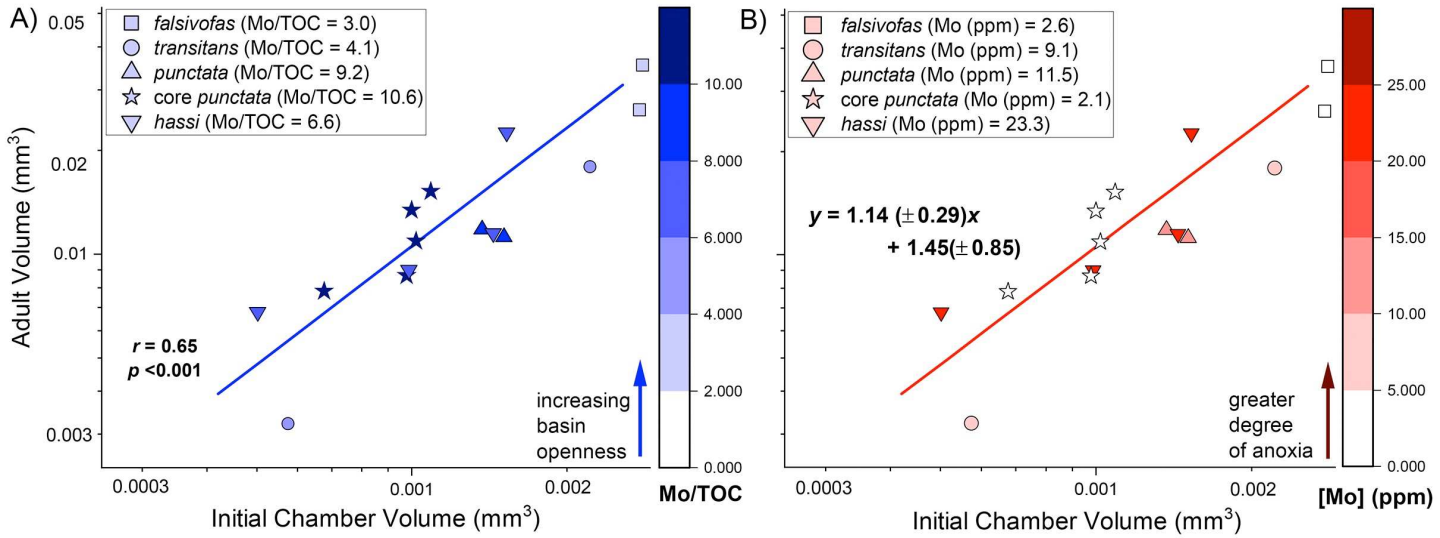
A)
B)
falsivofas (Mo/TOC = 3.0)
transitans (Mo/TOC = 4.1)
punctata (Mo/TOC = 9.2)
core punctata (Mo/TOC = 10.6)
hassi (Mo/TOC = 6.6)
falsivofas (Mo (ppm) = 2.6)
transitans (Mo (ppm) = 9.1)
punctata (Mo (ppm) = 11.5)
core punctata (Mo (ppm) = 2.1)
hassi (Mo (ppm) = 23.3)
r = 0.65
p <0.001
y = 1.14 (±0.29)x
+ 1.45(±0.85)
increasing basin openness
greater degree of anoxia
Adult Volume (mm3)
Initial Chamber Volume (mm3)
0.05
0.02
0.01
0.003
0.0003
0.001
0.002
Mo/TOC
[Mo] (ppm)
10.00
8.000
6.000
4.000
2.000
0.000
25.00
20.00
15.00
10.00
5.000
0.000

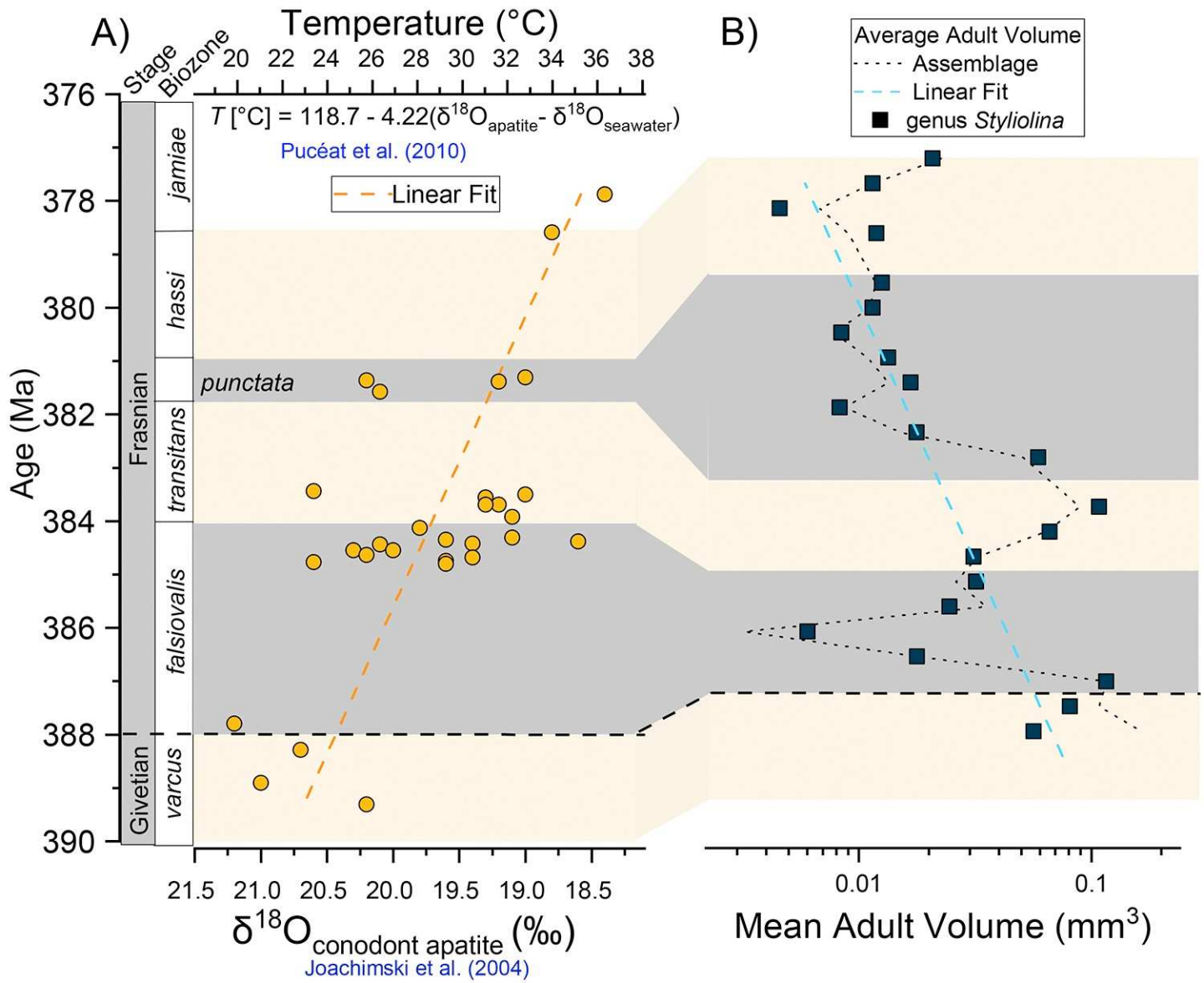
A)
Temperature (°C)
Stage
Biozone
20 22 24 26 28 30 32 34 36 38
T [°C] = 118.7 - 4.22(δ18Oapatite - δ18Oseawater)
Pucéat et al. (2010)
Linear Fit
Age (Ma)
376
378
380
382
384
386
388
390
Frasnian
Givetian
jamiae
hassi
punctata
transitans
falsiovalis
varcus
21.5 21.0 20.5 20.0 19.5 19.0 18.5
δ18Oconodont apatite (‰)
Joachimski et al. (2004)
B)
Average Adult Volume
Assemblage
Linear Fit
genus Styliolina
0.01
0.1
Mean Adult Volume (mm3)

TABLE 1. STRATIGRAPHIC AND LITHOLOGIC DESCRIPTION OF STUDIED SECTIONS

Stage	Group	Formation	Description	Depositional environment
Givetian	Hamilton Group	Windom Shale Member (Moscow Formation)	Thinly bedded gray shale with irregularly spaced silty limestone beds, articulate brachiopods	Calm, shallow marine
Frasnian	Genesee Group	North Evans Limestone	Bone bed with a matrix of black and gray limestone and shale	Shallow-water lag deposit
		Genundewa Limestone	Nodular to shaley irregularly bedded styliolinid grainstone	Condensed pelagic facies under sediment-starved conditions
		West River Shale Formation	Dark gray shale and siltstone	Deep basin
	Sonyea Group	Middlesex Shale Formation	Basal-meter fissile black pyritic shale grades into gray shale	Suboxic deep basin
		Cashaqua Formation	Light greenish-grey shale with numerous concretionary horizons, dark shale interbeds	Slow sedimentation, shallow marine
	West Falls Group	Rhinestreet Shale Formation	Black shales with minor siltstones	Moderately deep suboxic basin
		Angola Shale	Bioturbated light to dark gray shale, numerous concretionary horizons	Shallow marine

TABLE 2. STATISTICAL SUMMARY FOR EVOLUTIONARY MODELING OF LOG-TRANSFORMED MEAN ADULT VOLUMES

Model	No. of parameters	Parameter values*	Akaike information criterion (AIC) score (AICc)†	AICc weight percent (wt%)§
Unbiased random walk	2	$i_0 = 1.32$ $\sigma^2_{step} = 0.08$	15.2	24.9
Directional random walk	3	$i_0 = 1.32$ $\mu_{step} = 0.026$ $\sigma^2_{step} = 0.08$	17.8	7.1
Ornstein-Uhlenbeck process	4	$i_0 = 1.29$ $\alpha = 0.67$ $\sigma^2_{step} = 0.19$ $\theta = 2.00$	13.2	68.1

*At each discrete time interval, starting at initial value i_0, an increment of evolutionary change is drawn from a Gaussian distribution with mean step size μ_{step} and variance σ^2_{step}. For unbiased random walks $\mu_{step} = 0$, so that it has only 2 free parameters. A positive μ_{step} indicates an increase in trait value over time. For the Ornstein-Uhlenbeck process, θ is the position of the phenotypic optimum value with a restoring force of α at each step interval. Because the data are log transformed, all parameter values are unitless.

†To correct for small sample number, a modified Akaike Information score, AICc, is used. When the number of observations, N, is less than 40 times the number of free parameters, K, then AICc = AIC +(2K[K+1]/N–K–1), where AIC is equal to the negative 2 times log-likelihood (l) plus twice the number free parameters, or AIC = –2l +2K (Hunt, 2006; Hunt et al., 2008).

§Akaike weight percent (AICc wt%) is a convenient way of comparing model fit and involves rescaling the AICc scores so that the weight's sum to 1 and the value represents the relative support of each model to the data. The weight percent of each AICc, w_i, score is given as $w_i = \exp(-1/2\Delta_i)/\Sigma_j \exp(-1/2\Delta_j)$ (Hunt, 2006).